Estimation-informed, Resource-aware Robot Navigation for Environmental Monitoring Applications

Lonnie T. Parker, Richard A. Coogle, Ayanna M. Howard
School of Electrical and Computer Engineering
Georgia Institute of Technology
Atlanta, GA 30332
lonnie@gatech.edu, rcoogle3@gatech.edu, ayanna@ece.gatech.edu

***Abstract*— Environmental monitoring of spatially-distributed geo-physical processes (e.g., temperature, pressure, or humidity) requires efficient sampling schemes, particularly, when employing an autonomous mobile agent to execute the sampling task. Many approaches have considered optimal sampling strategies which specialize in minimizing estimation error, while others emphasize reducing resource usage, yet rarely are both of these performance parameters used concurrently to influence the navigation. This work discusses how a spatial estimation process and resource awareness are integrated to generate an informed navigation policy for collecting useful measurement information. We also enable a direct comparison between this informed navigation method and more common approaches using two performance metrics. We show that our informed navigation outperforms these approaches based on performance evaluation as a function of estimation error and resource usage for a useful range of coverage within the sampling area.**

***Index Terms*— Earth-observing systems (EOS), robotic survey system (RSS), inertial measurement unit (IMU).**

I. Introduction

In an effort to increase the information gain of Earth-observing systems (EOS), it is necessary to integrate robotic technology into different geodetic frameworks currently deployed [1]. In the past decade, robotic surveying has surfaced repeatedly as a reliable measurement tool for collecting measurements of different geo-physical processes (e.g., elevation, humidity, pressure or temperature), particularly in remote or hazardous locations [2], [3], [4]. Other applications, including precision farming and mapping of natural gases, have also found success employing mobile robotics to conduct surveying (or sampling) tasks [5], [6]. Given their prevalence, we determine navigation strategies which enhance a mobile agent's ability to autonomously select useful samples [7]. Our work considers the task of using a mobile agent to collect science samples for spatial reconstruction of environmental phenomena. This paper provides a contrast between the reconstruction error achieved (from collected samples) using specific navigation policies and the resources required to execute those policies. We introduce an informed navigation scheme driven by specific parameters in situ, allowing the mobile agent to make sampling decisions that yield low reconstruction error while requiring minimal resources.

II. Background

Previous efforts have focused on efficiently quantifying the performance of a sampling task based on reduced reconstruction error generated from collected samples. The resources required to execute that task are, however, rarely considered concurrently in the performance evaluation, i.e., when making sampling decisions, reducing error matters, but not cost. Rahimi, et al. uses very specific sampling policies, including a variant of stratified random sampling [6], but does not consider the physical resources for completing the sampling task, e.g., battery or time of experiment. As a complementary example, Tunstel et al. also addresses robotic sampling within the context of planetary surveying. In their work, they specify a quality of performance (QoP) metric to quantify the navigation schemes that are the least resource-intensive, yet does not address sampling scientific data to yield accurate spatial models [8].

When constrained to collecting a limited number of samples, solutions are developed as pre-planned site surveys. Many robotic approaches to environmental monitoring employ spatially static patterns as solutions for sampling data, i.e., the sampling locations are pre-determined [9]. Specifically, Spike, et al., and others [5], [10], emphasize the usefulness of the "lawnmower" motion such that the trajectory of the mobile agent outlines a series of evenly spaced swaths and collected samples are taken along the path traversed. Alternatively, a spatially random sampling distribution would achieve an improvement in coverage [11], yet, the widespread placement of samples requires increased resources to navigate to each sampling location. While these options may considerably reduce resources or improve reconstruction, independently, there are a lack of navigation strategies for sampling that are driven by them both, collectively. We enable the direct contrasting of reconstruction error and resources achieved by multiple navigation strategies employed for environmental sampling. We also demonstrate the preferability of one strategy over others specifically designed to account for these two performance parameters.

III. Approach

Several elements are required to fully outline the theory in our work. In Section III-A, we discuss the unique nature of the phenomena from which we are interested in collecting samples and how it differs from other approaches. In Section III-B, we introduce the theory behind the metrics used to evaluate our informed navigation algorithm, relative to

baseline strategies proposed in this work. We conclude with Section III-C, formally outlining the method of navigation used to collect information from the sample space and how it relates to the metrics outlined.

A. Sampling Environment

We first discretize our environment to define physical constraints on the boundaries of where our mobile agent will navigate. The entire sample space is defined by $S = X_{dim} \times Y_{dim}$, where $X_{dim} = [0, \delta, \ldots, \delta(M-1)]$, and $Y_{dim} = [0, \delta, \ldots, \delta(N-1)]$. M and N represent the number of rows and columns of samples along the x and y dimensions, respectively, and δ is the user-defined spatial resolution. Additionally, for all x_i belonging to X_{dim} and for all y_j belonging to Y_{dim}, there exists a sample from the terrain, $z(s_{i,j})$. Let $s_{i,j} = (x_i, y_j)$ for $i \in 1:M$ and $j \in 1:N$.

Many environments are modeled mathematically as a set of real-valued functions, Z, defined in $\mathbb{R}^2$. We quantize this set of functions into a dual-class set of functions as our ground truth, re-labeling the new quantized set, F (Figure 1). This representation of environmentally-monitored data is

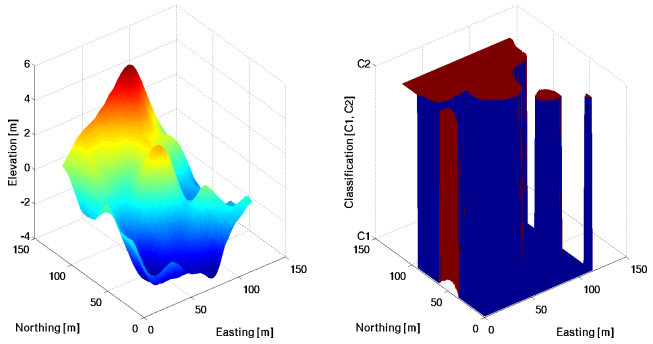

Fig. 1: Quantization of example function z (left) into analogous dual-class function f (right).

supported by geostatistical literature, particularly in instances when only the absence or presence of data is required as a measurement [12]. We use a mobile agent to execute each navigation strategy to collect samples of this data. An example scenario is chemical monitoring and measuring whether or not sample locations exhibit a toxicity level that exceeds a pre-defined maximum. The set, C, represents the possible values within the dual-class system to which each sample in S can belong, where $C = [c_1, c_2]$. For each function, z, from the set Z, we assign a threshold to define the classification of values at all corresponding sample locations, subsequently defining a new function, f, and new values, $f(s_{i,j})$, for all $s_{i,j}$ (Equation (1)).

$$f = \begin{cases} c_1 & \text{if } z > \bar{z} \\ c_2 & \text{if } z \leq \bar{z} \end{cases} \tag{1}$$

We will investigate the methods by which a mobile agent collects a set of B samples from one of these functions, f, according to different navigation algorithms. Our goal is to design an algorithm A that enables the reconstruction of a function, $\hat{f}_A$, such that f is approximated with some minimal amount of error and requires minimal resources to collect B samples.

B. Robotic Performance Metrics

When reconstructing spatially distributed data with an autonomous (or remote) sampling robot, two parameters are most dominant for evaluating performance of the sampling task executed, i.e., reconstruction error and resource usage. The former is an assessment of how samples collected will be processed to generate an accurate spatial model of the phenomena, while the latter associates a cost with the accuracy achieved. In the context of robotics and dynamic sensor selection, different work highlights spatial interpolators specifically designed for continuously-valued data within a space. In some cases, these spatial interpolators are chosen only to estimate samples off line [6], whereas in other cases, they are selected specifically to influence the sample selection process in real time [13]. Throughout the design of our navigation/sampling strategy discussed in this paper, we perform the latter, designing our navigation decisions around a dual-class interpolator as an example estimator for data represented as belonging to one of two classes (Section III-A). To the authors' knowledge, this is the first example of such an algorithm designed for collecting data within a dual-class environment.

For the entire space, S, we label a set of B total sampled locations as s. We also label the complementary set of $MN - B$ unsampled locations as $\hat{s}$, such that $(s \cup \hat{s}) = S$. Our interpolator is inspired by a set of L-point nearest-neighbor rules analogous to kNN classification [14], enabling the estimation of information at all the $MN - B$ unsampled locations.

The estimation of a value at an unknown location, $\hat{s}_{i,j}$, for example, is determined by the values at and proximity to neighbor locations, each identified as $s_{k,l}$. From this, we generate an expected error for each unsampled location and therefore a total expected error associated with the unique configuration, q. This configuration, q, is one of Q_B possible configurations for B samples in the space.

$$\hat{f}_A(\hat{s}_{i,j}) = \begin{cases} c_1 & \text{if } \sigma_{c_1} > \sigma_{c_2} \\ c_2 & \text{if } \sigma_{c_1} < \sigma_{c_2} \\ w(\rho) & Otherwise \end{cases} \tag{2}$$

In Equation (2), $\hat{f}_A(\hat{s}_{i,j})$ generates an estimate at the unobserved location $\hat{s}_{i,j}$ using samples acquired according to A. We select ρ as a uniform random variable defined between 0 and 1 and the function $w(\rho)$ to generate an estimate in the event that σ_{c_1} equals σ_{c_2}. We set the output of $w(\rho)$ equal to c_1 if $\rho < \gamma$ and c_2 if $\rho \geq \gamma$, where γ is defined between 0 and 1. Both of the values, σ_{c_1} and σ_{c_2}, are variables weighted based on the likelihood that the estimate at $\hat{s}_{i,j}$ belongs to one class versus the other (Equations (3)-(4)).

$$\sigma_{c_1} = \frac{u_1}{L}[1 - \frac{d_{c_{1,Avg}}}{R}] \tag{3}$$

$$\sigma_{c_2} = \frac{u_2}{L}[1 - \frac{d_{c_{2,Avg}}}{R}] \tag{4}$$

$$\eta = |\sigma_{c_1} - \sigma_{c_2}| \tag{5}$$

The values, $d_{c_{1,Avg}}$ and $d_{c_{2,Avg}}$, are the average proximities measured between all L nearest neighboring samples and the estimated location, $\hat{s}_{i,j}$, that belong to classes c_1 and c_2, respectively. The weights, u_1 and u_2, bias $\hat{f}_A(\hat{s}_{i,j})$, so that the unsampled location is assigned a value most similar to known samples surrounding it and $u_1 + u_2 = L$. The value R represents a maximum distance between an estimate and its neighbors. We define the value η as a confidence measure in each estimated value from $\hat{s}$ (Equation (5)). Finally, to assess actual error, $error_q^{Actual}$, Equation (6) allows us to contrast our estimation associated with a sampling configuration, q, with ground truth data, f.

$$error_q^{Actual} = \frac{\sum_{g=1}^{MN-B} \epsilon_g}{MN - B} \tag{6}$$

$$\epsilon_g = \begin{cases} 0 & \text{if } \hat{f}_A(\hat{s})_g = f(\hat{s})_g \\ 1 & \text{if } \hat{f}_A(\hat{s})_g \neq f(\hat{s})_g \end{cases} \tag{7}$$

The second performance parameter, resource usage, is quantified using average nearest neighbor distance for sampling configuration q [11]. The metric, d_b^{NN}, is calculated by averaging the distances of each sample in q from its nearest neighbor (Equation (8)).

$$D_{Avg}^{NN} = \frac{\sum_{b=1}^{B} d_b^{NN}}{B} \tag{8}$$

This measure is a raw cost associated with a specific configuration yielding a specific error. Resources are calculated based on a ratio of the average nearest-neighbor distance for the given configuration and a maximum possible average nearest-neighbor distance, D_{Max}^{NN} (Equation 9) [15].

$$Resources = 100 * \frac{D_{Avg}^{NN}}{D_{Max}^{NN}} \tag{9}$$

Both metrics (reconstruction error and resources) are combined to produce a quantitative understanding of how a sampling configuration, resulting from one particular navigation scheme, fares against another (Figure 2). Each diamond

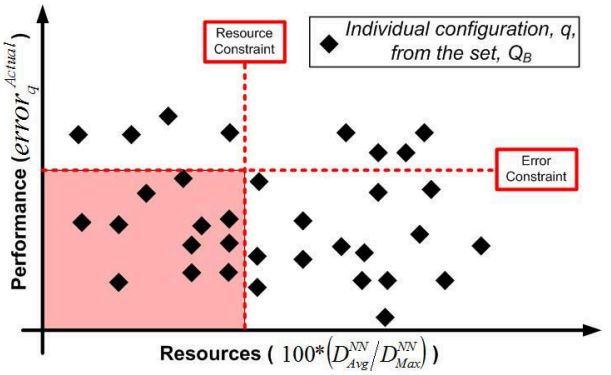

Fig. 2: A pictorial representation of how individual sampling configurations, q, can be compared in terms of performance metrics, reconstruction error and resources.

shown in Figure 2 represents a unique sampling configuration, q, from Q_B. The error and resource constraints are user-specific and aid a scientist in selecting the most appropriate navigation algorithm. We introduce our unique method of generating these configurations via navigation in the next section.

C. Intelligent Sampling for Navigation

Previous work in sampling spatially-distributed phenomena, given certain assumptions, has produced many intelligent navigation options [16], [17]. As discussed in Section II, we re-introduce the navigation solutions that serve as a baseline, providing the context in which our specific algorithm has made improvements.

To generate an even distribution of samples within an area, we turn to traditional lawnmower navigation, referred to hereafter as lawnmower-traditional [5], [10]. By directing navigation in a back-and-forth motion, the desired spatial allocation of samples is achieved. Additionally, this navigation policy is conservative in the amount of required resources, due to the uniformity in the agent's trajectory between samples. In contrast, requiring greater resources, but potentially achieving greater reconstruction accuracy, we also employ a lawnmower-random navigation. This navigation allows the collection of samples at varying distances from each other within the sample space, introducing an element of randomness to the way a mobile agent moves between subsequent samples [18], [19].

We can leverage the benefits of spatially-diverse sampling, commonly achieved by randomized patterns, while also conservatively considering the resources necessary to complete the navigation task, as seen with a lawnmower-based structure. We introduce lawnmower-informed navigation, influenced by the theory in Section III-B, to intelligently collect samples at locations that will yield lower reconstruction error while actively reducing required resources.

Based upon scientists' requirements for a given survey, we designate a finite number of evenly-spaced reference swaths (and consequently B samples to be collected) a priori. If, for example, the measurement device (e.g., altimeter or spectrometer) can only be deployed aboard the mobile agent long enough to allow collection of B samples, then that limitation will map to a specific number of reference swaths. An agent navigates along each swath as a reference, of either length M or N (Section III-A), adjusting its heading based on a custom function. This function, r_s, uses two parameters calculated at each time step, $\eta_{s'}^{min}$ and $d_{s'}$, to determine which sample, from a subset of candidate samples, will serve as the next navigation waypoint, and therefore sampling location (Algorithm 1). This type of navigation is considered a greedy approach [20], since a global goal is not sought. The algorithm only selects the sample that best satisfies 1) low error (based on a low average estimation confidence) and 2) low resources, i.e., the closest sample to the current location at an individual time step (Figure 3-5). While we note that the error is priviledged relative to resources as a metric, the contribution to the Earth scientist is the ability to give one metric preferential treatment over another for

Algorithm 1 Navigation function, r_s

Require: Candidate set of subsequent sampling locations, s'.
$\sigma_{c_1}^{s'}$ {Class 1 membership weights}
$\sigma_{c_2}^{s}$ {Class 2 membership weights}
$d_{s'}$
for $j \leq size(s')$ **do**
$\eta_{s'}(j) = |\sigma_{c_1}^{s'} - \sigma_{c_2}^{s'}|$
end for
$\eta_{s'}^{min} = min(\eta_{s'})$
if $size(min(\eta_{s'})) > 1$ **then**
From the remaining available samples with $\eta_{s'}^{min}$, select closest sample according to $d_{s'}$.
end if
return {(x,y) location of best sample according to $\eta_{s'}^{min}$ and $d_{s'}$.}

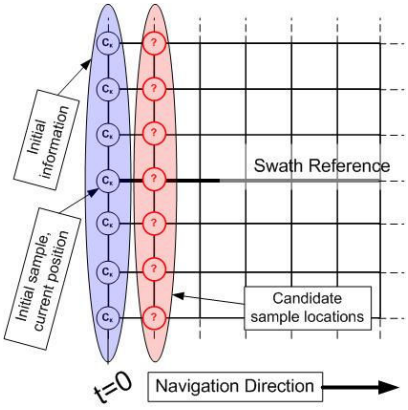

Fig. 3: Initial scene for sample selection.

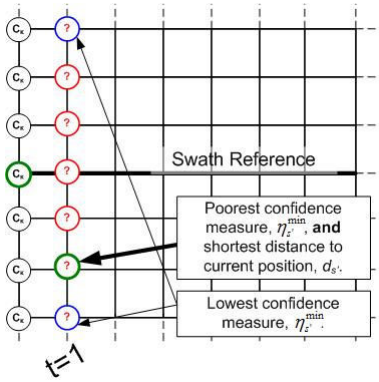

Fig. 4: Identify potential sample locations, from a local subset, with lowest confidence measure, $\eta_{s'}^{min}$.

determining their desired navigation strategy as a sampling scheme [15].

IV. Results

We evaluate our lawnmower-informed navigation (Section III-C) with respect to two navigation methods (lawnmower-traditional and lawnmower-random), illustrating how the most suitable sampling scheme can be selected, specifically according to the performance metrics of reconstruction error and resource usage.

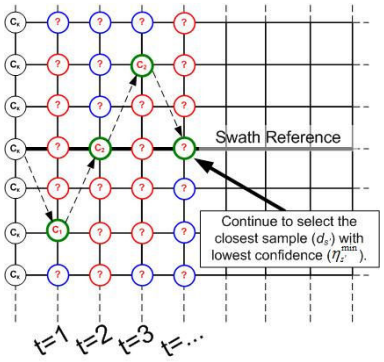

Fig. 5: Identify potential sample locations, from a local subset, with lowest confidence measure, $\eta_{s'}^{min}$, located closest to current location based on $d_{s'}$.

A. Simulation Trials

To demonstrate the success of our lawnmower-informed navigation algorithm, we generated 100 simulated dual-class data maps, using a custom DEM maker in MATLAB® [21]. Recall from Section III-A, that our proposed navigation is exclusively designed to assist with the collection of threshold-relevant (or dual-class) data, i.e., data that falls above or below a pre-defined scientific threshold (Figure 1). We selected elevation as our primary phenomenon and our simulation tool enabled us to produce terrain maps exhibiting realistic features found in nature, e.g., hills and valleys. We subsequently applied a threshold (the statistical mean, $\bar{z}$) to the value of each sampling location within S. Each location is, thus, defined as belonging to class c_1 or c_2 depending on whether the elevation value at a particular location, $z(s_{i,j})$, is below or above $\bar{z}$, respectively.

We chart the reconstruction error of each unique sampling configuration (generated by each navigation algorithm) as a function of its corresponding resource usage for multiple percent coverages (Figure 6). There are 100 unique sample configurations, representing the output from applying these navigation schemes to our data maps. For a majority of coverages tested, the lawnmower-informed navigation consistently generates configurations that lead to lower reconstruction error than lawnmower-traditional and lawnmower-random. Additionally, lawnmower-informed navigation consistently required fewer resources than lawnmower-random navigation for coverages less than 15 percent (Figure 6). There exists a gradual shift to the right for the sampling configurations produced by lawnmower-informed, indicating an increase in required resources as coverage increases. We attribute this increase to a physical limitation in the amount of spatial diversity that can be exhibited by different navigation schemes, according to a lawmower-based framework. This limitation is discussed more in [15].

B. In-field trials

Using the SECT-II platform (`www.bluebotics.com`), we performed an informal topographical survey to obtain a realistic terrain model for testing the navigation algorithms.

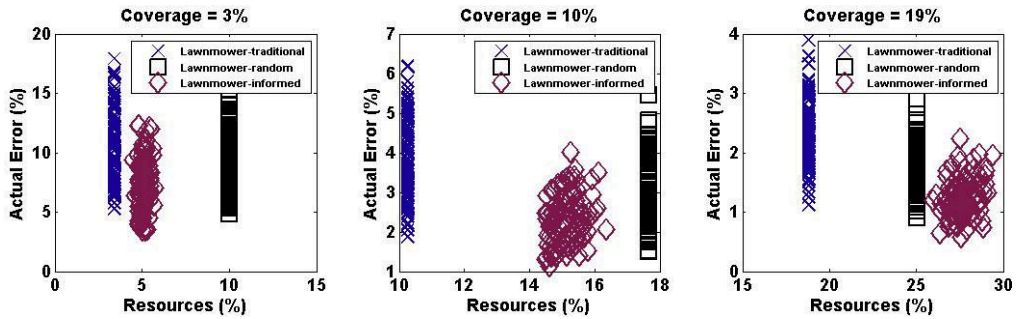

Fig. 6: Comparison of algorithms as a function of error and resource metrics for as applied to simulated DEM data.

We equipped the mobile unit with several commercially available devices for data collection and processing including an inertial measurement unit and microcontroller that enabled wireless communication with and operation of the SECT-II. Specifically, the SECT-II was mounted with a low-cost dual-axis accelerometer (ADXL322) that provided resolutions of 8.31 [mV/degree] and 8.38 [mV/degree] for each axis, x and y, respectively. To process this inertial data, a Connex 400XM (`www.gumstix.com`) with a 400MHz ARM processor, wireless 802.11g ethernet, and bluetooth capabilities were integrated with the sensing suite. A Robostix board provided an analog-to-digital converter (ADC) unit for conversion of continuous analog voltages from the ADXL322 into useful inertial measurements (Figure 7). With

(a) Test site for field trials.

(b) SECT-II robotic platform with accompanying sensors and processing.

Fig. 7: Robotic survey system testing.

the relevant tilt measurements collected, we derived a digital elevation map corresponding to a section of a local park to consider the impact of a physically-realizable space on our navigation strategies. From the continuous, raw elevation data acquired, we repeated trials of each navigation strategy on a quantized, i.e., dual-class, version of the real terrain produced from our survey. We, again, use elevation as our measured phenomena, collecting data at locations where the elevation detected falls below or exceeds the statistical mean of all elevations within the testing space, S.We repeat analysis of how each navigation algorithm performs on this single terrain, a real data map and confirm an improvement in our performance metrics when using lawnmower-informed navigation to dictate sample selection (Figure 8). This improvement is consistent with our results from Section IV-A. The graphic shown in Figure 8 is further validated with tabulated

TABLE I: Relevant performance and resource data for navigation strategies applied to realistic DEM data at specific coverages.

	Coverage (%)	Error (%)	Resources (%)
Lawnmower-traditional		5.841	2.563
Lawnmower-random	2	4.786	8.721
Lawnmower-informed		3.134	4.477
Lawnmower-traditional		3.109	4.541
Lawnmower-random	4	2.866	11.752
Lawnmower-informed		1.612	7.609
Lawnmower-traditional		2.328	7.670
Lawnmower-random	7	1.746	15.328
Lawnmower-informed		1.035	12.341
Lawnmower-traditional		1.756	12.403
Lawnmower-random	12	0.871	20.268
Lawnmower-informed		0.786	18.263
Lawnmower-traditional		1.756	16.440
Lawnmower-random	16	0.766	23.529
Lawnmower-informed		0.453	22.540
Lawnmower-traditional		1.224	24.254
Lawnmower-random	24	0.756	28.704
Lawnmower-informed		0.353	29.961

data confirming the balance of improved performance metrics for lawnmower-informed navigation versus lawnmower-traditional or lawnmower-random (Table I). Consistent with our simulation results from Section IV-A, for coverages less than 15 percent, lawnmower-informed navigation required less resources than lawnmower-traditional and lawnmower-random, while selecting samples that generated the lowest reconstruction error for our realistic terrain model. Furthermore, this improvement provides strong evidence for the value in incorporating both the estimation theory (planned for use off line following sample collection) and greedy resource conditions to inform the navigation of a robotic sampling system.

V. Conclusions and Future Work

This work has shown the benefit of incorporating an estimation methodology with resource-awareness for sampling decisions into a navigation strategy for a robotic survey system (RSS). With respect to scale, we anticipate that, should this experiment be considered for a larger space, i.e. several orders of magnitude greater, the need for a robotic sampling agent would not be as great and scientists could rely more heavily on remote sensing capabilities. If, however,

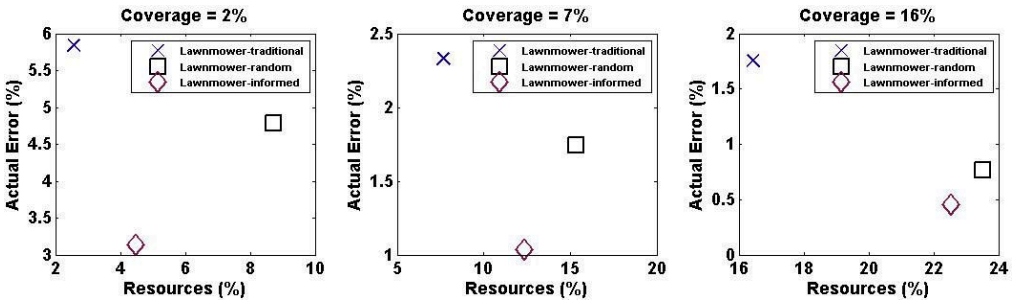

Fig. 8: Comparison of algorithms as a function of error and resource metrics for as applied to realistic DEM data.

the monitored area of interest is occluded, such that in situ sampling is the only viable option, we consider our work to scale well, provided a sufficient discretization of the space. Another issue is the robustness of this work given a temporally-dynamic phenomena. All examples considered in this work were presumed temporally-static, thus a major step forward will include designing methods that account for changes across the spatially-distributed phenomena studied. Of foremost importance is the integration of localization and sampling error. We did not account for these types of errors within our framework, considering our simulation environment as error free, but future runs with this update will generate more interesting statistical work. Future work also includes updating the estimation process to account for the spatial variability of the dual-class data being sampled, i.e., spatial frequency of the data sampled from one adjacent location to another. It is expected that expanding this work to consider spatial frequency will assist in quantifying the performance limitations on our lawnmower-informed navigation and any subsequent navigation designed to include the estimation process and resource usage concurrently.

ACKNOWLEDGMENTS

The authors wish to thank the Science, Mathematics and Research for Transformation (SMART) Program for funding of this work.

REFERENCES

[1] *Precise Geodetic Infrastructure: National Requirements for a Shared Resource*. Washington, DC: The National Academies Press, 2010.

[2] J. Lever, A. Streeter, and L. Ray, "Performance of a solar-powered robot for polar instrument networks," in *Proceedings of the 2006 IEEE Int. Conference on Robotics and Automation*, Orlando, Florida, May 2006, pp. 4252–4257.

[3] T. W. Fong, M. Bualat, L. Edwards, L. Flueckiger, C. Kunz, S. Y. Lee, E. Park, V. To, H. Utz, N. Ackner, N. Armstrong-Crews, and J. Gannon, "Human-robot site survey and sampling for space exploration," in *AIAA Space 2006*, September 1996.

[4] D. Apostolopoulos, M. D. Wagner, B. Shamah, L. Pedersen, K. Shillcutt, and W. R. L. Whittaker, "Technology and field demonstration of robotic search for antarctic meteorites," *Int. Journal of Robotics Research*, Dec 2000.

[5] J. Jin, "Optimal field coverage path planning on 2d and 3d surfaces," PhD Dissertation, Iowa State University, Department of Agricultural and Biosystems Engineering, 2009.

[6] M. Rahimi, R. Pon, W. J. Kaiser, G. S. Sukhatme, D. Estrin, and M. Srivastava, "Adaptive sampling for environmental robotics," in *IEEE Int. Conference on Robotics and Automation*, New Orleans, LA, 2004.

[7] L. T. Parker and A. M. Howard, "Real-time robotic surveying for unexplored arctic terrain," in *NASA Earth Science Technology Forum*, June 22 – 24 2010.

[8] E. Tunstel, J. Dolan, T. W. Fong, and D. Schreckenghost, "Mobile robotic surveying performance for planetary surface site characterization," in *Performance Evaluation and Benchmarking of Intelligent Systems*, E. Tunstel and E. Messina, Eds. Springer, August 2009.

[9] V. B. Spikes and G. S. Hamilton, "Glas calibration-validation sites established on the west antarctic ice sheet," in *International Symposium on Remote Sensing of Environment*, Honolulu, Hawaii, 2003.

[10] B. S. Bourgeois, D. L. Brandon, J. J. Cheramie, and J. Gravley, "Efficient hydrographic survey planning using an environmentally adaptive approach," in *DoD Technical Report*, Stennis Space Center, MS, 2006.

[11] P. J. Clark and F. C. Evans, "Distance to nearest neighbor as a measure of spatial relationships in populations," *Ecology*, vol. 35, no. 4, pp. 445 –453, October 1954.

[12] R. Webster and M. A. Oliver, *Geostatistics for Environmental Scientists*. John Wiley & Sons Publishing, 2003.

[13] C. Guestrin, A. Krause, and A. Singh, "Near-optimal sensor placements in Gaussian processes," in *International Conference on Machine Learning (ICML)*, August 2005.

[14] T. Cover and P. Hart, "Nearest neighbor pattern classification," *Information Theory, IEEE Transactions on*, vol. 13, no. 1, pp. 21 –27, january 1967.

[15] L. Parker, "Science-centric sampling approaches of geo-physical environments for realistic robot navigation," PhD Dissertation, Georgia Institute of Technology, School of Electrical and Computer Engineering, 2012.

[16] M. H. Rahimi, M. Hansen, W. Kaiser, G. S. Sukhatme, and D. Estrin, "Adaptive sampling for environmental field estimation using robotic sensors," in *IEEE/RSJ International Conference on Intelligent Robots and Systems*, Aug 2005, pp. 747–753.

[17] K. H. Low, J. M. Dolan, and P. Khosla, "Adaptive multi-robot wide-area exploration and mapping," in *Proceedings of the 7th Int. Joint Conference on Autonomous Agents and Multiagent Systems-Volume 1*, 2008, p. 2330.

[18] B. P. Marchant and R. M. Lark, "Optimized sample schemes for geostatistical surveys," *Mathematical Geology*, vol. 39, no. 1, pp. 113–134, 2007.

[19] O. O. Ayeni, "Optimum sampling for digital terrain models: A trend towards automation," *Photogrammetric Engineering and Remote Sensing*, vol. 48, no. 11, pp. 1687–1694, 1982.

[20] A. Stentz, "The focussed d* algorithm for real-time replanning," in *In Proceedings of the International Joint Conference on Artificial Intelligence*, 1995, pp. 1652–1659.

[21] H. Mei, L. T. Parker, and A. M. Howard, "Conversion of gis contour maps into surface digital elevation models," in *IEEE Int. Conference on Systems, Man, and Cybernetics*, Anchorage, AK, October 2011.